ACTA CHEMICA SCANDINAVICA 20 (1966) 2865–2879

On the Tellurides of Nickel

JAN BARSTAD, FREDRIK GRØNVOLD, ERLING RØST and EGIL VESTERSJØ

Kjemisk institutt A, Universitetet i Oslo, Blindern, Oslo 3, Norway

Nickel tellurium alloys have been prepared and studied by means of X-ray, metallographic, pycnometric and magnetic methods. The following phases have been found:

The β-phase with composition from $NiTe_{0.667}$ to $NiTe_{0.692}$ when quenched from 580°C has a monoclinic crystal structure in the nickel-rich region (a = 7.551, b = 3.800, c = 6.100 Å, β = 91.22°) and an orthorhombic structure in the tellurium-rich region (a = 7.541, b = 3.795, c = 6.051 Å). The unit cell of Ni_3Te_2 contains 6 nickel and 4 tellurium atoms. With increasing tellurium content nickel vacancies are created. The structure of slowly cooled $NiTe_{0.69}$ and $NiTe_{0.70}$ is tetragonal ($a = 2 \times 3.781$, c = 6.077 Å for $NiTe_{0.69}$). The crystal structures of samples belonging to the β-phase region are apparently related to the $Cu_{4-x}Te_2$-Rickardite-structure.

The structure of Ni_3Te_2 changes to face centered cubic (a = 5.760 Å) between 850 and 900°C.

The γ-phase with composition between $NiTe_{0.77}$ and $NiTe_{0.775}$ has an orthorhombic structure (a = 3.912, b = 6.872, c = 12.375 Å for $NiTe_{0.77}$). The unit cell content is 10.4 nickel atoms and 8 tellurium atoms.

The δ-phase with composition from $NiTe_{1.09}$ to $NiTe_{2.00}$ has a hexagonal structure of the NiAs–$Cd(OH)_2$ type. The lattice constants vary continuously from a = 3.9686, c = 5.3620 Å for $NiTe_{1.09}$ to a = 3.8547, c = 5.2610 Å for $NiTe_{2.00}$. Density measurements support the view that the structure is of NiAs-like type with cation vacancies.

Magnetic measurements of the nickel tellurides are reported for temperatures in the range −183 to 450°C. The samples show very weak and nearly temperature independent paramagnetism.

A compound of nickel and tellurium was first prepared by Fabre,[1] who obtained the monotelluride in a metallic grey, crystalline form by heating the elements under nitrogen. Larger amounts of the compound were prepared by Tilden [2] for heat capacity measurements. Tibbals, Jr.[3] got a black precipitate with assumed composition $Ni_2Te_3 \cdot 4H_2O$ by adding an aqueous solution of sodium telluride to a solution containing nickel acetate and acetic acid. The precipitate yielded NiTe when heated in hydrogen. Brukl [4] performed similar experiments and apparently obtained NiTe without heating the precipitate.

The crystal structure of NiTe was reported by Oftedal [5] as being of the NiAs-($B8$)-type. Tengnér [6] prepared $NiTe_2$ and found it to have a structure of the $Cd(OH)_2$-$C6$-type. A sample with composition Ni_2Te_3 was also found to have hexagonal structure and unit cell dimensions intermediate between those of NiTe and $NiTe_2$. The region NiTe to $NiTe_2$ was studied in more detail by Klemm and Fratini [7] by X-rays, density and magnetic measurements. They found a decrease in the lattice constants with increasing tellurium content, but the results were not entirely reproducible.

Schneider and Imhagen [8] have measured lattice constants of samples in the region NiTe to $NiTe_2$ at various temperatures up to 800°C. Further lattice constant data for samples in the region NiTe to $NiTe_{1.95}$ were reported by Shchukarev and Apurina.[9] Continuous variations in lattice constants, corresponding to a range of homogeneity between the above limits, were observed. Vapour pressure measurements of tellurium-rich samples by Westrum and Machol [10] indicated the limiting composition of the phase to be $NiTe_{1.9}$ at 712°C. Evidence for NiTe being a two phase product consisting of the $Ni_{1+x}Te_2$ phase ($0 < x < 1$) and a more nickel-rich phase with a complex superstructure, was presented by Dvoryankina and Pinsker [11] in an electron diffraction study of thin nickel telluride films.

Magnetic susceptibility measurements in the range NiTe to $NiTe_2$ by Klemm and Fratini [7] showed weak, temperature independent paramagnetism, in some cases slightly field strength dependent. Galperin and Perekalina [12] measured the magnetic susceptibility of NiTe and found it to be very low and decreasing slightly with increasing temperature. Nickel tellurides have been studied magnetically by Uchida and Kondoh [13] over a wide range of composition and temperature. They interpreted the data in terms of a ferromagnetic phase with composition $NiTe_{0.33}$ and a paramagnetic phase with composition above $NiTe_{0.7}$.

As result of an isopiestic investigation at 900°C Shchukarev and Apurina [9] suggested the existence of three nickel-rich phases, one with composition $NiTe_{0.62}$, one with a composition range from $NiTe_{0.66-0.67}$ to $NiTe_{0.82-0.83}$, and one with composition $NiTe_{0.88}$. No crystallographic data were given. Further electron diffraction work by Dvoryankina and Pinsker [14] confirmed the presence of a phase with approximate composition Ni_3Te_2. Two different structures were observed and their relationships discussed.

The only nickel telluride mineral known is melonite. Peacock and Thompson [15] examined X-ray powder photographs of melonite and an alloy with composition $NiTe_2$ and found the lattice dimensions to be nearly identical. It was concluded that melonite had a structure of the cadmium hydroxide type and the composition $NiTe_2$.

One object of our study was to obtain more exact information about the phase region NiTe to $NiTe_2$ and the structural changes involved. In addition, the phases and structures of more nickel-rich samples were to be considered. Some of the results date several years back,[16] and they will here be integrated with results of more recent studies.

EXPERIMENTAL

The alloys were prepared by heating appropriate mixtures of the elements in evacuated and sealed quartz tubes. Metallic nickel was prepared from "Nickel oxide, low in cobalt and iron" from the British Drug Houses, Ltd. by reduction with purified and dried hydrogen gas at temperatures up to 1000°C. A spectrographic analysis showed only the presence of traces of copper and magnesium as impurities. The tellurium used in the earlier experiments was "Tellurium metal lumps" from the British Drug Houses, Ltd. purified by repeated vacuum distillations in quartz apparatus. A spectrographic analysis of the final product showed less than 0.01 % iron, and only traces of aluminium, magnesium, and lead as impurities. In later experiments "Special high-purity semiconductor grade tellurium" (99.999 %) from the American Smelting and Refining Company was used.

Samples containing less than 56.5 at. % tellurium were in most cases heated to fusion and then annealed at about 580°C for 3 to 5 days. After quenching or cooling to room temperature the samples were finely crushed and homogenized. One series of samples was heated at 580°C for one week in small quartz tubes and quenched in water, while another series of samples was kept at 450°C for one month and quenched, and a third series of samples cooled to room temperature during a period of two days.

X-Ray studies of the samples were made in Debye-Scherrer cameras of 11.48 cm diameter with asymmetric film mounting, a Guinier-type focussing camera of 8 cm diameter with strictly monochromatized Cu$K\alpha_1$ radiation, a 19 cm diameter Unicam high-temperature camera and a Weissenberg camera. The lattice constants are expressed in Ångström units on the basis of λ (Cu$K\alpha_1$) = 1.54051 Å, or a KCl standard, taking a = 6.2919 Å at 20°C. The probable errors in the lattice constants given are judged to be ± 0.02 % for the hexagonal structures and ± 0.04 % for the tetragonal, orthorhombic, and monoclinic structures. Lattice constants from earlier investigations, expressed in kX units, have been transformed to Å by multiplication by the factor 1.00202.

Densities of the samples were measured at 25°C by a vacuum pycnometric method using kerosene as displacement liquid. Each sample weighed approximately 2 g.

Magnetic susceptibilities were measured by the Gouy method at temperatures ranging from −183 to 450°C and at three different maximum field strengths of 4015, 4700, and 5110 Ørsteds, respectively.

RESULTS AND DISCUSSION

A. Phase analysis

A survey of the alloys prepared and the phases identified from X-ray photographs of the samples are given in Table 1.

The α-phase. Powder photographs of the samples $NiTe_{0.50}$ and $NiTe_{0.60}$ showed the presence of two phases, the α-phase, nickel, with lattice constant a = 3.524 Å, and a phase with previously unknown structure. The lattice constant of the α-phase is equal to that of pure nickel, a = 3.5238 Å (25°) according to Swanson and Tatge,[17] within the limits of experimental error. Thus, the solubility of tellurium in nickel appears to be small.

The β-phase. Metallographic and X-ray examinations of samples with composition $NiTe_{0.667}$ show the presence of one phase only, the β-phase. X-Ray reflections of corresponding lines are found at the same angles in $NiTe_{0.60}$ and $NiTe_{0.667}$, while reflections from nickel are observed in $NiTe_{0.60}$. A gradual change occurs in the range $NiTe_{0.667}$ to $NiTe_{0.70}$, indicating a variable composition of the β-phase in this region. In $NiTe_{0.70}$ small amounts of another phase is observed. After slow cooling of $NiTe_{0.69}$ and $NiTe_{0.70}$ to room temperature small changes in the X-ray patterns are noticeable compared to the results obtained for quenched samples.

Table 1. Composition of the samples studied and the phases observed after quenching from 450°C.

Composition		Phases	Composition		Phases
$NiTe_x$	At. % Te		$NiTe_x$	At. % Te	
Ni	0.00	α			
$NiTe_{0.50}$	33.33	$\alpha + \beta$	$NiTe_{1.075}$	51.81	$\gamma + \delta$
$NiTe_{0.60}$	37.50	$\alpha + \beta$	$NiTe_{1.09}$	52.15	δ
$NiTe_{0.66}$	39.76	$\alpha + \beta$	$NiTe_{1.10}$	52.38	δ
$NiTe_{0.667}$	40.00	β	$NiTe_{1.125}$	52.94	δ
$NiTe_{0.67}$	40.18	β	$NiTe_{1.15}$	53.49	δ
$NiTe_{0.68}$	40.48	β	$NiTe_{1.20}$	54.55	δ
$NiTe_{0.69}$	40.83	β	$NiTe_{1.30}$	56.52	δ
$NiTe_{0.70}$	41.18	$\beta + \gamma$	$NiTe_{1.40}$	58.33	δ
$NiTe_{0.725}$	42.00	$\beta + \gamma$	$NiTe_{1.50}$	60.00	δ
$NiTe_{0.739}$	42.50	$\beta + \gamma$	$NiTe_{1.60}$	61.54	δ
$NiTe_{0.75}$	42.86	$\beta + \gamma$	$NiTe_{1.70}$	62.96	δ
$NiTe_{0.76}$	43.18	$\beta + \gamma$	$NiTe_{1.80}$	64.29	δ
$NiTe_{0.77}$	43.50	$\beta + \gamma$	$NiTe_{1.90}$	65.52	δ
$NiTe_{0.775}$	43.66	$\gamma + \delta$	$NiTe_{1.95}$	66.10	δ
$NiTe_{0.78}$	43.82	$\gamma + \delta$	$NiTe_{2.00}$	66.67	δ
$NiTe_{0.79}$	44.13	$\gamma + \delta$	$NiTe_{2.05}$	67.21	$\delta + \varepsilon$
$NiTe_{0.80}$	44.44	$\gamma + \delta$	$NiTe_{2.50}$	71.43	$\delta + \varepsilon$
$NiTe_{0.90}$	47.37	$\gamma + \delta$	$NiTe_{32.3}$	97.00	$\delta + \varepsilon$
$NiTe_{1.00}$	50.00	$\gamma + \delta$	Te	100.00	ε

X-Ray photographs of $NiTe_{0.667}$ taken in a high temperature camera show that a change in structure has taken place at 900°C. The high temperature phase is not retained on quenching, but characteristic differences are observed under the microscope of polished samples quenched from 900 and 850°C, respectively.

The γ-phase. Increasing amounts of a new phase are observed in samples with composition from $NiTe_{0.70}$ to $NiTe_{0.77}$. In $NiTe_{0.775}$ the β-phase is no longer visible, but the γ-phase is here in equilibrium with another nickel telluride phase with higher tellurium content. Slight shifts in line positions are observed for the γ-phase, indicating a range of homogeneity within the limits $NiTe_{0.77}$ and $NiTe_{0.775}$.

The δ-phase. A mixture of the γ- and δ-phases is observed in samples with composition from $NiTe_{0.775}$ to $NiTe_{1.075}$, whereas $NiTe_{1.09}$ contains lines from the δ-phase only. Gradual changes in line positions on the X-ray photographs occur from $NiTe_{1.09}$ to $NiTe_{2.00}$. Reflections from tellurium are found in the photograph of $NiTe_{2.05}$. To explore the solubility of nickel in tellurium a sample with 97 at. % tellurium was prepared. After heating the sample at 580°C for one week and quenching it, large, thin flakes of the δ-phase were observed in polished sections under the microscope. No such flakes were observed after quenching the sample from 800°C. Thus, liquid tellurium seems to dissolve at least 3 at. % nickel at 800°C, but considerably less at 580°C. The solubility decreases rapidly with decreasing temperature and

is determined [10] to be 0.3 at. % nickel at the measured eutectic temperature 449°C.

B. Crystal structures

The β-phase. Some crystals of the β-phase were obtained after annealing $NiTe_{0.68}$ at 580°C for about two months. On the basis of cell dimensions derived from oscillation and Weissenberg photographs complete indexing of the Guinier photographs of the powdered samples could be performed. In the nickel-rich part of the homogeneity range the structure is monoclinic. The indexing of a photograph of $NiTe_{0.667}$, or Ni_3Te_2, is found in Table 2, and the lattice constants are listed in Table 3. A change in structure from monoclinic to orthorhombic is observed when the tellurium content of the phase exceeds $NiTe_{0.68}$. Data obtained for $NiTe_{0.69}$, see Table 4, and for $NiTe_{0.70}$ suggested halving of the *a*-axis value observed in the monoclinic region, but that was disproved by the many weak reflections *hkl* with $h = 2n + 1$ present on Weissenberg photographs of $NiTe_{0.69}$. It is remarkable, however, that four reflections on the powder photograph of $NiTe_{0.69}$ remain unexplained. Since these reflections were not found on the Weissenberg photographs, considerable doubt exist with regard to their origin.

In Fig. 1 the lattice constants of the β-phase are plotted as function of composition. All three axes contract with increasing tellurium content, and the monoclinic deformation disappears, as already mentioned, near the composition $NiTe_{0.68}$. Assuming the quenching to be effective, the homogeneity

Table 2. X-Ray powder data of Ni_3Te_2, quenched from 580°C. Cu$K\alpha_1$-radiation.

I_{obs}	$\sin^2\theta \times 10^5$ obs	calc	*h k l*	I_{obs}	$\sin^2\theta \times 10^5$ obs	calc	*h k l*
w	1039	1040	1 0 0	m	14456	14434	2 1 $\bar{2}$
w+	1592	1595	0 0 1	m	14864	14874	2 1 2
vw	2576	2581	1 0 $\bar{1}$	vw	15563	15564	1 0 3
w	2685	2691	1 0 1	st	16446	16434	0 2 0
w	5136	5150	1 1 0	st	16663	16658	4 0 0
w+	5652	5650	2 0 $\bar{1}$	w	18183	18192	2 0 $\bar{3}$
st	5707	5704	0 1 1	m	18461	18466	0 1 3
m−	5864	5870	2 0 1			18473	4 0 1
m	6385	6381	0 0 2	w	18848	18852	2 0 3
w	6688	6690	1 1 $\bar{1}$	w	22095	22094	2 2 $\bar{1}$
vw	6794	6800	1 1 1	w	22140	22141	4 1 $\bar{1}$
w	7305	7312	1 0 $\bar{2}$	w	22301	22291	2 1 $\bar{3}$
st	8283	8276	2 1 0			22294	2 2 1
m	9775	9758	2 1 $\bar{1}$	w	22592	22582	4 1 1
m+	9975	9978	2 1 1			22596	4 0 $\bar{2}$
vw	10335	10325	2 0 $\bar{2}$	w	22805	22815	0 2 2
w	10498	10490	0 1 2	w	22950	22960	2 1 3
w−	11145	11131	3 0 1	w	23227	23220	3 0 $\bar{3}$
vw	11424	11421	1 1 $\bar{2}$	w	23490	23479	4 0 2
vw	11622	11640	1 1 2	vw	23764	23746	1 2 $\bar{2}$
m	14363	14357	0 0 3	w	25539	25524	0 0 4

Table 3. Lattice constants (Å) of the β-phase after quenching from 580°C.

Sample	a	b	c	$\beta°$
$NiTe_{0.60}$	2 × 3.776	3.800	6.100	91.25
$NiTe_{0.667}$	2 × 3.775	3.800	6.100	91.22
$NiTe_{0.68}$	2 × 3.774	3.798	6.094	90.18
$NiTe_{0.69}$	2 × 3.772	3.796	6.073	90
$NiTe_{0.70}$	2 × 3.771	3.795	6.065	90
$NiTe_{0.725}$	2 × 3.771	3.795	6.065	90

Table 4. X-Ray powder data of $NiTe_{0.69}$ quenched from 580°C. Cu$K\alpha_1$-radiation.

I_{obs}	$\sin^2\theta \times 10^5$ obs	calc	$h\ k\ l$	I_{obs}	$\sin^2\theta \times 10^5$ obs	calc	$h\ k\ l$
w−	1360	—	—	m	14488	14479	0 0 3
w+	1602	1609	0 0 1	vst	14712	14705	2 1 2
w−	2347	—	—	st−	16440	16440	0 2 0
w−	4843	—	—	st−	16640	16640	4 0 0
st	5723	5719	0 1 1	m−	18590	18599	2 0 3
st	5770	5769	2 0 1	st	22218	22209	2 2 1
st−	6436	6435	0 0 2	st	22363	22360	4 1 1
w−	7081	—	—	w	22739	22749	2 1 3
st	8269	8270	2 1 0	w+	22870	22875	0 2 2
st+	9887	9895	2 1 1	w+	23076	23075	4 0 2
w+	10556	10545	0 1 2	m	25737	25740	0 0 4
w+	10594	10595	2 0 2				

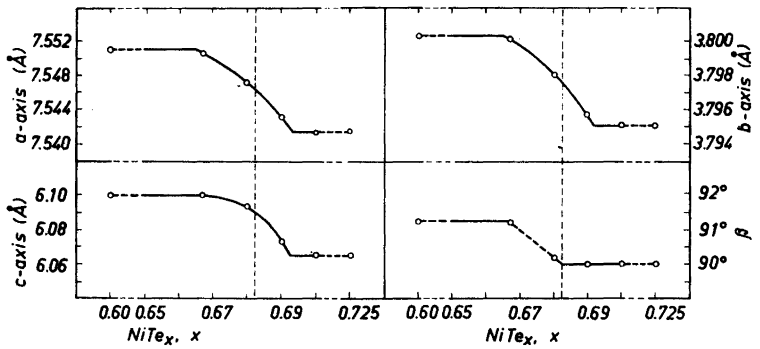

Fig. 1. Lattice constants (Å) of the β-phase as function of composition $NiTe_x$. Dashed vertical lines indicate the composition at which the symmetry changes from monoclinic to orthorhombic.

range of the β-phase at 580°C extends between the limits $NiTe_{0.667}$ and $NiTe_{0.692}$, or 40.00 and 40.90 at. % tellurium.

The structures encountered so far for the β-phase are pseudo-tetragonal, but it is possible to obtain a purely tetragonal structure by slow cooling of $NiTe_{0.69}$ and $NiTe_{0.70}$ from 450°C over a period of two days. Quenching the samples from 330°C did not result in a tetragonal structure. Powder photograph data for $NiTe_{0.70}$ are given in Table 5. No lines from the γ-phase are found in the slowly cooled sample. The resulting lattice constants are listed in Table 6. A slight increase in the c-axis is noticeable from $NiTe_{0.70}$ to $NiTe_{0.69}$, while $NiTe_{0.68}$ seems to be a two-phase product with monoclinic $NiTe_{0.67}$ as the other phase. The lattice constants of $NiTe_{0.667}$ quenched and $NiTe_{0.67}$ slowly cooled are equal within the limits of experimental error.

The densities of $NiTe_{0.667}$ and $NiTe_{0.69}$ have been measured as 8.168 and 8.126 g cm^{-3}, respectively. The values correspond to six (6.02) nickel atoms and four (4.01) tellurium atoms in the unit cell of $NiTe_{0.667}$ and 5.80 nickel atoms and 4.00 tellurium atoms in $NiTe_{0.69}$. Thus, an increasing number of vacant nickel sites are created as the tellurium content of the γ-phase increases.

The three different structures of the β-phase found so far are obviously closely related to each other, and show striking resemblances to the structure

Table 5. X-Ray powder data of $NiTe_{0.70}$, slowly cooled to room temperature. Cu$K\alpha_1$-radiation.

I_{obs}	$\sin^2\theta \times 10^5$ obs	calc	$h\,k\,l$	I_{obs}	$\sin^2\theta \times 10^5$ obs	calc	$h\,k\,l$
w+	1029	1037	1 0 0	w−	15086	15093	3 2 1
w+	1597	1608	0 0 1	st+	16597	16597	4 0 0
m−	2632	2645	1 0 1	vw	18178	18205	4 0 1
w	5191	5187	2 1 0	m	18615	18623	2 0 3
vst	5762	5757	2 0 1	vw	19248	19242	4 1 1
m+	6430	6433	0 0 2	st	22362	22354	4 2 1
w	6788	6794	2 1 1	w	22772	22773	2 2 3
w	7462	7467	1 0 2	m−	23043	23030	4 0 2
st	8302	8299	2 2 0	w+	25731	25731	0 0 4
st	9909	9906	2 2 1	w	27194	27179	4 2 2
m−	10564	10579	2 0 2	m−	30085	30082	5 2 1
vw	13483	13485	3 2 0	st−	31080	31071	4 0 3
m−	14475	14474	0 0 3				
vst−	14737	14731	2 2 2				

Table 6. Lattice constants (Å) of the β-phase after slow cooling.

Sample	a	b	c	$\beta°$
$NiTe_{0.66}$	2 × 3.776	3.801	6.098	91.18
$NiTe_{0.67}$	2 × 3.774	3.799	6.099	91.15
$NiTe_{0.68}$	2 × 3.776	3.792	6.099	91.20
	2 × 3.783	(2 × 3.783)	6.078	90
$NiTe_{0.69}$	2 × 3.781	(2 × 3.781)	6.077	90
$NiTe_{0.70}$	2 × 3.781	(2 × 3.781)	6.074	90

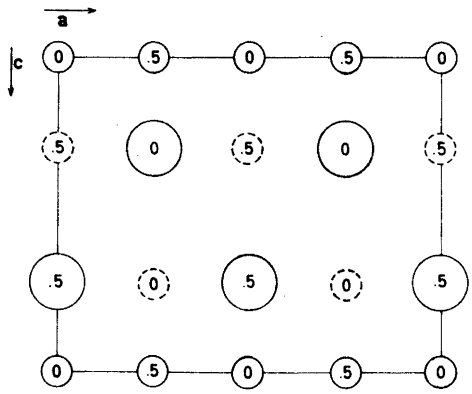

Fig. 2. Projection of the Rickardite-like structure along (010). Large circles indicate tellurium atoms and small circles the metal atoms. Partly occupied nickel sites are indicated by dashed circles.

of Rickardite, $Cu_{4-x}Te_2$ with $x = 1.2$, as determined by Forman and Peacock.[18] The structure can be described as being of the Fe_2As-C38-type, but with a large fraction of the metal atoms missing, or of the PbO-*B*10-type with a large fraction of interstitial metal atoms. A projection of two unit cells of the Rickardite structure along (010) is shown in Fig. 2.

The fully drawn circles represent the arrangement in the *B*10-type structure, with tellurium atoms as large circles and nickel atoms as small ones. The dashed circles indicate additional metal positions occupied in the C38-type structure, but empty in the *B*10-type. For Rickardite, $Cu_{2.8}Te_2$, Forman and Peacock [18] concluded that the extra (0.8) copper atom was distributed at random over the equivalent positions in the unit cell. Judging from the closely constant intensity ratio between the reflections from the $Cu_{2.8}Te_2$ structure and the $Ni_{3.00-2.86}Te_2$ substructure, the structures of the β-phase apparently involve related ordering schemes for the interstitial nickel atoms. Work on these structures is being continued.*

Table 7. High-temperature powder photograph data for Ni_3Te_2 at 900°C. Cu$K\alpha$ radiation.

I_{obs}	$\sin^2\theta \times 10^5$ obs	calc	$h\,k\,l$	I_{obs}	$\sin^2\theta \times 10^5$ obs	calc	$h\,k\,l$
m	5371	5364	1 1 1	st−	19687	19667	3 1 1
m−	7151	7152	2 0 0	vw	21443	21455	2 2 2
st	14295	14303	2 2 0	vw	28593	28606	4 0 0

* *Added in proof:* In a preliminary communication by Kok, R.B., Wiegers, G.A. and Jellinek, F. (*Rec. Trav. Chim. Pays Bas* **84** (1965) 1585) the structures of the β-phase are discussed and ordering schemes for the monoclinic and tetragonal superstructures suggested. Lattice constants for the γ-phase, which agree with those found here are also reported, but the composition of the γ-phase is given as $NiTe_{0.9}$.

In Ni_3Te_2 a phase transformation takes place around 850°C, resulting in a face-centered cubic structure with lattice constant $a = 5.760$ Å at 900°C. The powder photograph data are given in Table 7. Similar high-temperature phases have been encountered in the nickel-sulfur system by Liné and Huber [19] and in the nickel-selenium system by Grønvold, Møllerud and Røst.[20] The latter phases have extended ranges of homogeneity, but this has not yet been investigated for the telluride phase. Anyhow, the composition $NiTe_{0.62}$ given for the most nickel-rich telluride at 900°C by Shchukarev and Apurina [9] might well correspond to the nickel-rich limit of the homogeneity range of the high-temperature phase.

The γ-phase. Weissenberg photographs of a crystallite of the γ-phase showed a primitive orthorhombic structure. The Guinier photograph of $NiTe_{0.77}$ could be indexed as shown in Table 8. Slight differences are present between lattice constants for $NiTe_{0.77}$ and $NiTe_{0.775}$; see Table 9. With increasing tellurium content the *a*- and *b*-axes expand a little, while the *c*-axis contracts. The homogeneity range of the γ-phase is obviously very narrow since the photograph of $NiTe_{0.77}$ contains reflections from the β-phase and that of $NiTe_{0.775}$ contains reflections from the δ-phase.

A density determination of $NiTe_{0.77}$ gave $d = 8.107$ g cm^{-3}, which corresponds to 10.35 nickel atoms and 7.97 tellurium atoms per unit cell. No isostructural compounds have apparently been described. It should be noted, however, that in the electron diffraction study of thin nickel telluride films by Dvoryankina and Pinsker [14] two different structures with related lattice periodicities in the basal plane were found. One structure was indexed on the basis of hexagonal structure with dimensions $a = 6.72 \pm 0.01$ Å, $c = 20.2 \pm 0.1$ Å, the other on the basis of a rhombohedral pseudo-cell with $a_1 = a/\sqrt{3} = 3.88$ Å and $c_1 = c = 20.2$ Å (hexagonal orientation). No exact composition of the

Table 8. X-Ray powder data of $NiTe_{0.77}$ quenched from 580°C. Cu$K\alpha_1$-radiation.

I_{obs}	$\sin^2\theta \times 10^5$ obs	calc	*h k l*	I_{obs}	$\sin^2\theta \times 10^5$ obs	calc	*h k l*
w−	1558	1550	0 0 2	w	10073	10076	1 0 4
vw	1647	1643	0 1 1	w	11339	11332	1 1 4
w	5435	5427	1 0 2	w	12391	12389	1 2 3
m	5521	5520	1 1 1	vst	14716	14711	0 2 5
w	5728*	—	—	vst	14821	14819	1 1 5
m−	5775*	—	—	st	15182	15183	1 3 0
m+	6199	6199	0 0 4	st	15510	15510	2 0 0
m+	6578	6575	0 2 2	w	16459*	—	—
st	6680	6683	1 1 2	w	16672*	—	—
vw	8279*	—	—	vw	18663	18670	1 3 3
w	8514	8512	0 2 3	w	18987	18997	2 0 3
m+	8626	8620	1 1 3				
m	9290	9289	1 2 1				
w	9904*	—	—				

* Reflections from the β-phase.

Table 9. Lattice constants (Å) of the γ-phase as measured on two-phase samples on either side of the homogeneity range.

Sample	a	b	c
$NiTe_{0.77}$	3.912	6.872	12.38
$NiTe_{0.775}$	3.921	6.875	12.37

Table 10. Lattice constants (Å) and cell volume (Å^3) of the δ-phase for samples with composition from NiTe to $NiTe_{2.05}$.

NiTe	Ni_yTe_2	At. % Te	a	c	c/a	V
$NiTe_{1.00}$	$Ni_{2.000}Te_2$	50.00	3.9687	5.3624	1.3512	73.146
$NiTe_{1.075}$	$Ni_{1.861}Te_2$	51.81	3.9685	5.3614	1.3510	73.125
$NiTe_{1.09}$	$Ni_{1.835}Te_2$	52.15	3.9686	5.3620	1.3511	73.138
$NiTe_{1.10}$	$Ni_{1.818}Te_2$	52.38	3.9665	5.3632	1.3521	73.077
$NiTe_{1.125}$	$Ni_{1.778}Te_2$	52.94	3.9577	5.3653	1.3557	72.781
$NiTe_{1.15}$	$Ni_{1.739}Te_2$	53.49	3.9541	5.3668	1.3573	72.667
$NiTe_{1.20}$	$Ni_{1.667}Te_2$	54.55	3.9419	5.3667	1.3614	72.220
$NiTe_{1.30}$	$Ni_{1.538}Te_2$	56.52	3.9208	5.3636	1.3680	71.406
$NiTe_{1.40}$	$Ni_{1.429}Te_2$	58.33	3.9067	5.3559	1.3710	70.791
$NiTe_{1.50}$	$Ni_{1.333}Te_2$	60.00	3.8922	5.3426	1.3726	70.092
$NiTe_{1.60}$	$Ni_{1.250}Te_2$	61.54	3.8824	5.3307	1.3730	69.585
$NiTe_{1.70}$	$Ni_{1.176}Te_2$	62.96	3.8716	5.3115	1.3719	68.952
$NiTe_{1.80}$	$Ni_{1.111}Te_2$	64.29	3.8652	5.2944	1.3698	68.500
$NiTe_{1.90}$	$Ni_{1.053}Te_2$	65.52	3.8605	5.2784	1.3673	68.127
$NiTe_{1.95}$	$Ni_{1.026}Te_2$	66.10	3.8567	5.2690	1.3662	67.871
$NiTe_{2.00}$	$Ni_{1.000}Te_2$	66.67	3.8547	5.2610	1.3648	67.700
$NiTe_{2.05}$	$Ni_{0.976}Te_2$	67.21	3.8547	5.2605	1.3647	67.693

phase (termed the β-phase) was given by Dvoryankina and Pinsker,[14] but it shows more resemblance to the γ-phase reported here than to the β-phase.

The δ-phase. The unit cell dimensions of the hexagonal δ-phase have been determined for several compositions and the results are given in Table 10. For these samples, annealed at 450°C and cooled to room temperature over a period of two days, the δ-phase extends between the limits $NiTe_{1.09}$ and $NiTe_{2.00}$, or 52.15 to 66.67 at. % tellurium. While the a-axis decreases regularly with increasing tellurium content, the c-axis goes through a maximum at about 54 at. %.

In Fig. 3 the lattice constants are plotted against composition, expressed as Ni_yTe_2. Values by earlier investigations are also included in Fig. 3. The data by Shchukarev and Apurina [9] are in good accord with those reported here, but the constancy in the region $NiTe_{1.00}$ to $NiTe_{1.09}$, indicating nonstoichiometry of the δ-phase, was missed. The c/a ratio shows rather small variations with the tellurium content, and the cell volume changes in a practically linear

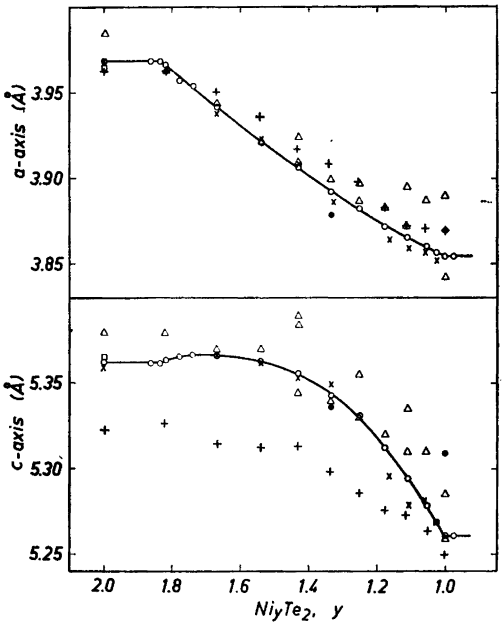

Fig. 3. Lattice constants (Å) of the hexagonal NiAs—$Cd(OH)_2$-type structure as function of composition Ni_yTe_2. ○: present study, □: Oftedal,[5] ●: Tengnér,[6] △: Klemm and Fratini,[7] +: Schneider and Imhagen,[8] ×: Shchukarev and Apurina.[9]

fashion when plotted against composition as Ni_yTe_2, with y varying from 1.84 for $NiTe_{1.09}$ to 1.00 for $NiTe_{2.00}$.

Results of the density measurements in the region of the δ-phase are found in Table 11. They confirm the presence of two tellurium atoms in the unit cell at all compositions and the corresponding increase in empty nickel

Table 11. Observed and calculated densities (g cm^{-3}) of the δ-phase.

Sample	d_{calc}	d_{obs}	Sample	d_{calc}	d_{obs}
$NiTe_{1.00}$	8.457	8.113	$NiTe_{1.40}$	7.952	7.864
$NiTe_{1.075}$	8.274	8.118			7.896
$NiTe_{1.10}$	8.223	8.112	$NiTe_{1.50}$	7.899	7.851
		8.138	$NiTe_{1.60}$	7.840	7.794
$NiTe_{1.125}$	8.202	8.098	$NiTe_{1.70}$	7.808	7.748
$NiTe_{1.15}$	8.163	8.039	$NiTe_{1.80}$	7.766	7.702
		8.076			7.723
$NiTe_{1.20}$	8.116	8.011	$NiTe_{1.90}$	7.725	7.690
		8.048	$NiTe_{1.95}$	7.716	7.653
$NiTe_{1.30}$	8.033	7.916	$NiTe_{2.00}$	7.698	7.662
		7.960	$NiTe_{2.05}$	—	7.628

sites from 0.16 to 1.00 when the composition of the phase goes from $NiTe_{1.09}$ to $NiTe_{2.00}$. Densities calculated assuming stoichiometric occupancies are also found in Table 11. They are from 0.5 to 1.5 % higher than the observed values, which might indicate tellurium vacancies. The differences could also be due to the presence of small voids in the crystal, unaccessible to the pycnometric liquid.

A break in the observed density *versus* composition curve, see Fig. 4, defines the nickel-rich composition limit of the δ-phase to be close to $NiTe_{1.1}$, in agreement with the X-ray results. Earlier density data by Klemm and Fratini [7] are also included in Fig. 4. They show a rather large spread, and are partly higher than those calculated assuming the presence of exactly two tellurium atoms per unit cell. No such irregularities have been observed in the present study.

The wide homogeneity range of the δ-phase, previously believed to extend between the exact compositions NiTe and $NiTe_2$, constitutes structurally the classic example of a transition from the NiAs-type structure to the $Cd(OH)_2$-type structure. In the idealized, hexagonal NiTe structure, space group $C6/mmc$ (D_{6h}^4), two nickel atoms occupy positions (a): 0,0,0; 0,0,$\frac{1}{2}$ and two tellurium atoms positions (d): 1/3, 2/3, 3/4; 2/3, 1/3, 1/4. The transition to the ditelluride is complete when one of the nickel positions, say 0,0,1/2, is vacant, while the 0,0,0 position remains occupied.

Powder photograph data of $NiTe_{1.15}$ and more tellurium-rich samples contain reflections hkl with $h-k = 3n$ and $l = 2n + 1$. Such reflections are forbidden in the NiAs-type structure, but allowed in the $Cd(OH_2)$-type structure, and might be taken as an indication of empty nickel sites in the 0,0,1/2 positions. Tendencies towards ordering of the vacancies and thus the formation of superstructures in annealed samples are to be expected, and the nickel-rich limit of the δ-phase might well be related to the stability of an ordered compound $Ni_{11}Te_{12}$ ($NiTe_{1.093}$). Indications of non-stoichiometry and super-

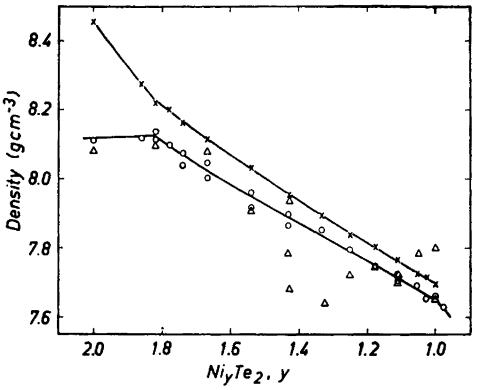

Fig. 4. Densities (g cm^{-3}) for samples in the δ-phase region. ○: observed, ×: calculated from X-ray data, △: observations by Klemm and Fratini.[7]

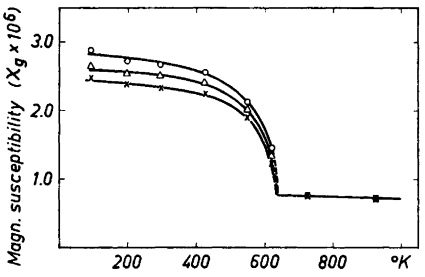

Fig. 5. Magnetic susceptibility *versus* temperature for $NiTe_{0.667}$ at three different field strengths; ○: 4015 Ø, △: 4700 Ø, ×: 5115 Ø.

structure formation have apparently also been found by Dvoryankina and Pinsker,[11] but no quantitative data are presented. The z-parameter of the tellurium atoms need not be exactly 1/4 (and 3/4) in the $Cd(OH_2)$-type structure, but Peacock and Thompson found it to be 0.250 ± 0.005 for synthetic $NiTe_2$. In the work by Dvoryankina and Pinsker [11] z was found equal to 0.253 with an R factor of 0.19.

Table 12. Interatomic distances (Å) in the structures of $NiTe_{1.10}$, $NiTe_{1.50}$, and $NiTe_{2.00}$.

$NiTe_{1.10}$	$NiTe_{1.50}$	$NiTe_{2.00}$
Ni–6Te = 2.654	Ni–6Te = 2.614	Ni–6Te = 2.585
Ni–1.6Ni = 2.681	Ni–0.7Ni = 2.671	–
Te–5.4Ni = 2.654	Te–4Ni = 2.614	Te–3Ni = 2.585
Te–6Te = 3.544	Te–6Te = 3.491	Te–6Te = 3.446
Te–6Te = 3.967	Te–6Te = 3.892	Te–6Te = 3.855

Interatomic distances in the structure of the δ-phase have been calculated for $NiTe_{1.10}$, $NiTe_{1.50}$, and $NiTe_{2.00}$ assuming ideal parameter values. As can be seen from Table 12 the distances change rather little with composition. Each nickel atom is surrounded by six tellurium atoms at the corners of a trigonal antiprism at distances ranging from 2.65 to 2.59 Å. It has in addition on the average 1.6 nickel atoms as nearest neighbours in the z-direction, 2.68 Å away at the composition $NiTe_{1.10}$, and none when the composition reaches $NiTe_{2.00}$. A slight decrease in the nickel-tellurium distances with increasing tellurium content is expected due to the lowering of the coordination numbers. Using the metallic radii by Pauling [21] the nickel-tellurium distances are calculated to be 2.684, 2.625, and 2.573 Å for $NiTe_{1.10}$, $NiTe_{1.50}$, and $NiTe_{2.00}$, respectively.

C. Magnetic properties

Magnetic susceptibility measurements have been carried out for different nickel telluride samples at six temperatures ranging from −183 to 450°C, and the results are given in Table 13. All samples except $NiTe_{0.667}$ show field strength independent susceptibilities and only the mean values for 4015, 4700, and 5115 Ørsteds are given in the Table.

For $NiTe_{0.667}$ the field strength dependence is still present at 300°C, but is absent at 450°C, see Fig. 5. Nickel has a ferromagnetic Curie temperature of 354°C according to Arajs,[22] and it thus seems reasonable to ascribe the slight ferromagnetism to minute quantities (< 0.01 %) of nickel present in the sample. It might either be due to incomplete reaction or to a slightly

Table 13. Magnetic susceptibilities ($\chi_g \times 10^6$) of the nickel tellurides at various temperatures.

	−183	−78	20	150	300	450°C
$NiTe_{0.667}$	*	*	*	*	*	0.77
$NiTe_{0.70}$	1.09	0.91	0.88	0.84	0.77	0.74
$NiTe_{0.78}$	1.17	0.65	0.52	0.56	0.55	0.55
$NiTe_{0.82}$	0.90	0.67	0.54	0.48	0.47	0.50
NiTe	0.71	0.63	0.58	0.55	0.54	0.54
$NiTe_{1.1}$	0.53	0.49	0.47	0.47	0.48	0.47
$NiTe_{1.15}$	0.52	0.46	0.43	0.42	0.43	0.43
$NiTe_{1.30}$	0.49	0.46	0.44	0.43	0.44	0.45
$NiTe_{1.50}$	0.35	0.37	0.34	0.36	0.37	0.35
$NiTe_{1.60}$	0.29	0.31	0.32	0.32	0.33	0.33
$NiTe_2$	0.43	0.34	0.28	0.26	0.23	0.22

* Weak, field strength dependent susceptibilities observed indicating the presence of traces of nickel in Ni_3Te_2.

higher composition limit of the β-phase, or to a variation in the phase limit with temperature.

In the work by Uchida and Kondoh [13] the Curie-temperature of the ferromagnetic alloys in the region Ni to $NiTe_{0.67}$ was found to increase from 650°K for $NiTe_{0.30}$ to 785°K for $NiTe_{0.65}$. This was interpreted in terms of a ferromagnetic phase in the region $NiTe_{0.33}$ to $NiTe_{0.67}$. No such phase has, however, been observed in the present study.

Reasonable agreement exists between the present results and those of Uchida and Kondoh for $NiTe_{0.70}$ at higher temperatures, but their values are about twice as high as ours at 90°K. The results reported by Galperin and Perekalina [12] for NiTe agree well with ours, while those by Uchida and Kondoh for NiTe, $NiTe_{1.20}$, and $NiTe_{1.50}$ are 20 to 30 % lower than the data reported here. The field strength dependence occurring for samples in the range NiTe to $NiTe_2$ in the work by Klemm and Fratini [7] has not been confirmed.

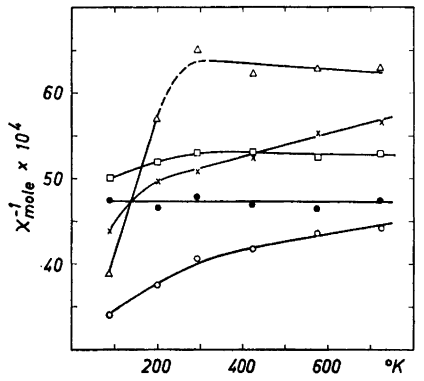

Fig. 6. Reciprocal susceptibilities per mole nickel *versus* temperature for different samples. ×: $NiTe_{0.78}$, △: $NiTe_{0.78}$, □: $NiTe_{1.10}$, ●: $NiTe_{1.50}$, ○: $NiTe_{2.00}$.

For all nickel telluride phases rather weak paramagnetism is encountered, with susceptibility values that are only slightly dependent upon temperature. The smallness of the values probably reflects collective nature of the nickel 3d electrons in the tellurides, rather than antiferromagnetism as has been assumed by earlier investigators. Inverse susceptibilities per mole nickel are shown in Fig. 6 after subtraction of induced diamagnetism in nickel (-17.7×10^{-6} mole^{-1} according to Asmussen [23]) and in tellurium (-70.6×10^{-6} mole^{-1} according to Angus [24]). Below room temperature the inverse susceptibilities curve downwards for all samples except $NiTe_{1.50}$. The effect is apparently most pronounced for the γ-phase and might indicate ferrimagnetic interactions at low temperatures.

Effective magnetic moments calculated according to the equation $\mu_{\text{eff}} = 2.83 \sqrt{\chi_{\text{mol}} \cdot T}\ \mu\text{B}$ are close to 0.4 μB at 90°K and increase to about 1.0 μB at 723°K for all samples. Very similar behavior has earlier been found [25] for nickel selenides in the range NiSe to $NiSe_2$, and it indicates the presence of both localized and collective electrons.

Acknowledgements. It is a pleasure to thank Professor Haakon Haraldsen for his interest in this study and for making laboratory facilities available. Miss Liv Gjertsen kindly carried out some of the magnetic measurements.

REFERENCES

1. Fabre, C. *Compt. Rend.* **105** (1887) 277.
2. Tilden, W. A. *Phil. Trans. Roy. Soc.* **203 A** (1904) 139.
3. Tibbals, Jr., C. A. *J. Am. Chem. Soc.* **31** (1909) 902.
4. Brukl, A. *Monatsh.* **45** (1924) 471.
5. Oftedal, I. *Z. physik. Chem.* **128** (1927) 135.
6. Tengnér, S. *Z. anorg. allgem. Chem.* **239** (1938) 126.
7. Klemm, W. and Fratini, N. *Z. anorg. allgem. Chem.* **251** (1943) 222.
8. Schneider, A. and Imhagen, K. H. *Naturwiss.* **44** (1957) 324.
9. Shchukarev, S. A. and Apurina, M. S. *Russ. J. Inorg. Chem. (English Transl.)* **5** (1960) 1167.
10. Westrum, Jr., E. F. and Machol, R. E. *J. Chem. Phys.* **29** (1958) 824.
11. Dvoryankina, G. G. and Pinsker, Z. G. *Kristallografiya* **7** (1962) 458.
12. Galperin, F. M. and Perekalina, T. M. *Dokl. Akad. Nauk. SSSR* **69** (1949) 19.
13. Uchida, E. and Kondoh, H. *J. Phys. Soc. Japan* **11** (1956) 21.
14. Dvoryankina, G. G. and Pinsker, Z. G. *Kristallografiya* **8** (1963) 556.
15. Peacock, M. A. and Thompson, R. M. *Univ. Toronto Studies, Geol. Ser.* **50** (1945) 63.
16. Barstad, J. *Thesis* University of Oslo 1954.
17. Swanson, H. E. and Tatge, E. *NBS Circular 539, vol.* **I** (1953) 13.
18. Forman, S. A. and Peacock, M. A. *Am. Mineralogist* **34** (1949) 441.
19. Liné, G. and Huber, M. *Compt. Rend.* **256** (1963) 3118.
20. Grønvold, F., Møllerud, R. and Røst, E. *Acta Chem. Scand.* **20** (1966) 1997.
21. Pauling, L. *J. Am. Chem. Soc.* **69** (1947) 542.
22. Arajs, S. *J. Appl. Phys.* **36** (1965) 1136.
23. Asmussen, R. W. *Magnetokemiske Undersøgelser over uorganiske Kompleksforbindelser*, København 1944.
24. Angus, W. R. *Proc. Roy. Soc. (London)* **A 136** (1932) 569.
25. Grønvold, F. and Jacobsen, E. *Acta Chem. Scand.* **10** (1956) 1440.

Received May 13, 1966.